Journal of Magnetic Resonance 272 (2016) 68–72

Contents lists available at ScienceDirect

Journal of Magnetic Resonance

journal homepage: www.elsevier.com/locate/jmr

Accelerating flow propagator measurements for the investigation of reactive transport in porous media

A.A. Colbourne, A.J. Sederman *, M.D. Mantle, L.F. Gladden

University of Cambridge, Department of Chemical Engineering and Biotechnology, Pembroke Street, Cambridge CB2 3RA, UK

ARTICLE INFO

Article history:
Received 20 July 2016
Revised 31 August 2016
Accepted 31 August 2016
Available online 1 September 2016

Keywords:
Reactive flow
MRI
NMR
Propagator
Rock
Dissolution
Porous media
Interpolation

ABSTRACT

NMR propagator measurements are widely used for identifying the distribution of molecular displacements over a given observation time, characterising a flowing system. However, where high q-space resolution is required, the experiments are time consuming and therefore unsuited to the study of dynamic systems. Here, it is shown that with an appropriately sampled subset of the q-space points in a high-resolution flow propagator measurement, one can quickly and robustly reconstruct the fully sampled propagator through interpolation of the acquired raw data. It was found that exponentially sampling ~4% of the original data-points allowed a reconstruction with the deviation from the fully sampled propagator below the noise level, in this case reducing the required experimental time from ~2.8 h to <7 min. As a demonstration, this approach is applied to observe the temporal evolution of the reactive flow of acid through an Estaillades rock core plug. It is shown that 'wormhole' formation in the rock core plug provides a channel for liquid flow such that the remaining pore space is by-passed, thereby causing the flow velocity of the liquid in the remaining part of the plug to become stagnant. The propagator measurements are supported by both 1D profiles and 2D imaging data. Such insights are of importance in understanding well acidisation and CO_2 sequestration processes.

1. Introduction

Pulsed field gradient (PFG)-NMR is a mature field, with a range of well-established techniques employed for the analysis of motion [1–3]. Of these, the implementation of PFG-NMR to acquire propagator measurements is particularly appropriate for the quantification of the range of velocities characteristic of flow through porous media which results from the tortuosity of the pore network [4,5]. Generated from the Fourier transform of the linearly ramped gradient dimension of a PFG-NMR experiment, a propagator is a probability distribution of signal amplitude versus displacement. For a distribution of moving spins, the signal amplitude (S) as a function of gradient strength ($\mathbf{g}$) is defined, using the q-space formalism ($\mathbf{q} = (2\pi)^{-1}\gamma\delta\mathbf{g}$), as:

$$S(\mathbf{q}) = \int P(\boldsymbol{R}, \Delta) \exp[2\pi i \mathbf{q}\boldsymbol{R}]\, d\boldsymbol{R}$$

the Fourier transform of which gives:

$$P(\boldsymbol{R}, \Delta) = \int S(\mathbf{q}) \exp[-2\pi i \mathbf{q}\boldsymbol{R}]\, d\mathbf{q}$$

where P is the probability that spins will move a distance $\boldsymbol{R}$ in the time Δ; γ is the gyromagnetic ratio and δ is the gradient pulse duration. Typically, displacement measurements are made in the superficial flow direction (R_z) with gradients being applied in the z-direction only. In the case of a fluid-saturated porous medium through which a fluid is flowing, one typically observes two different contributions to the propagator: stagnant spins, perhaps from fluid trapped in small or dead-end pores, and flowing spins, from fluid moving through connected pores [6]. Diffusion of the stagnant fluid within pores is usually well defined in the propagator, generating a sharp feature centred at zero displacement, the width of which is dominated by the self-diffusion coefficient of the fluid, corresponding to a broad attenuation in q-space. The range of displacements identified in the propagators associated with the flowing spins can span three or more orders of magnitude (typically from μm to mm), resulting in some broad features in the propagator and therefore a sharp feature at the centre of q-space. It follows that, to fully capture this range of displacements, one must sample with both a large enough range of q to avoid excessive truncation of the broad q-space diffusion signal and with high enough resolution in q to retain the detail of the sharp features of the signal from fast flowing molecules. The result is a PFG-NMR experiment with many gradient increments and an experimental time of hours; this poor

* Corresponding author.
E-mail address: ajs40@cam.ac.uk (A.J. Sederman).

http://dx.doi.org/10.1016/j.jmr.2016.08.018
1090-7807/

time resolution is an issue if the analysis of dynamic systems is desired.

Attempts to reduce the acquisition time for propagator measurements include non-uniform sampling, cumulant analysis, compressed sensing and real-space encoding using second order field gradients. For example, non-uniform sampling of propagator measurements has been demonstrated by Scheven et al. [7,8]. In that work, the data were sampled fully over the centremost 50% of the dataset, with 50% undersampling outside of this, reducing experimental time by 25%. Reconstruction was performed with linear interpolation. The technique was applied successfully under non-dynamic conditions in porous media. Alternatively where the full propagator is not required, cumulant analysis has been proposed in which acquisition time is reduced by acquiring sufficient data to determine the first three moments of the propagator efficiently [9,10]. Paulsen et al. [11] have demonstrated that 'compressed sensing' (CS) can be used to reconstruct sparsely sampled 2D and 3D diffusion propagator measurements, allowing sampling regimes with just 1.5% of the full data in the 3D case. CS requires that the reconstructed data can be sparsely represented in the transform domain. Paulsen et al. showed that both the first differential and wavelet transforms were sparse for a diffusion-dominated propagator. However, the propagators characteristic of the porous media of interest in the present work (i.e., rock cores) are not sparse in either of these domains due to the broad, smooth feature associated with flowing spins, and CS reconstruction in the commonly applied format cannot usefully be applied. Fast diffusion measurements have also been made with different gradient hardware in which the gradient strength varies with sample position, usually with a second order gradient variation [12,13]. In principle this could be applied to acquire propagators but would require a homogeneous sample since different q values are effectively acquired from different positions. This, along with the requirement for non-linear field variations, makes it impractical to apply to transport in rock core plugs, the application of interest in the present work.

Here it is shown that due to the form of the data characteristic of flow in a porous medium such as a rock core plug, q-space can be reliably reconstructed from ~4% of the fully sampled acquisition through the use of appropriate sampling schemes and standard interpolation techniques. We illustrate this approach by monitoring the evolving hydrodynamics caused by dissolution of a rock core plug with a reactive flow of hydrochloric acid where propagator evolution occurs on a timescale much shorter than that required for a fully sampled propagator measurement.

2. Materials and methods

NMR propagator and imaging experiments were conducted on an Estaillades (carbonate) rock core plug. First, fully sampled propagators were acquired under non-reactive flow conditions. These data were then used to explore the extent of undersampling that could be used to reconstruct the fully sampled dataset to within experimental error. Second, 1D profiles, 2D images and undersampled propagators were then acquired at regular time intervals during a reactive flow experiment.

A cylindrical rock core plug of the Estaillades carbonate of diameter and length 38 mm and 72 mm, respectively was saturated by evacuating the dry plug at ~300 Pa for 2–4 h, before the introduction of deionized water. The plug was then evacuated for further ~15 h. The core was then mounted in an Ergotech™ PEEK rock core flow cell with a confining pressure of 1.7 MPa [14]. Fluid was delivered to the rock core holder by a Quizix QX1500-HC dual cylinder syringe pump, controlled from a PC running the PumpWorks™ software. The confining pressure was applied using 3M Flourinert FC-43, which is NMR silent in typical ^{1}H chemical shift ranges, and maintained with a Gilson model 307 pump on a closed flow loop with a back pressure regulator. For the fully sampled propagator, deionized water was flowed at 10 mL min^{-1} (0.15 mm s^{-1} superficial velocity) for the duration of the experiment. For the dissolution experiment 0.01 M HCl (pH 2.0) was introduced at 10 mL min^{-1} over 15.5 h.

All NMR measurements were made using a Bruker BioSpin AV spectrometer with a 2 T horizontal bore superconducting magnet (85 MHz ^{1}H frequency) and a 60 mm diameter birdcage radiofrequency (RF) coil. Fully sampled propagators of the flow of deionized water through the rock core plug were acquired using 4 averages of a modified '13-interval' pulse sequence in which the final hard 180° RF pulse is replaced with a soft 180° pulse to allow slice selection, taking 2 h 51 min for the complete sampling of 1024 q-space points [15,16]. The acquisition parameters were as follows: observation time, Δ = 750 ms; gradient pulse duration, δ = 2.5 ms; and maximum applied magnetic field gradient strength, g_{max} = 10.5 G cm^{-1}. The flow gradient was aligned with the superficial flow direction. Data from a 5 mm thick section of core at the centre of the sample were taken to provide local propagator data and to avoid end effects caused by the entry and exit of fluid. The range of the q-space data and number of points sampled was chosen such that the broad diffusive signal was sampled at large q and that the increment in q-space was sampled at a high enough resolution to avoid 'foldover' of signal from the highest displacement spins occurring as the pore space became more heterogeneous throughout the experiment. In general, the number of points required can be estimated from the quotient of the maximum displacement possible and the displacement resolution required, typically given by half of the RMS displacement due to restricted diffusion. Where fewer points are acquired, propagators may still be produced but are more likely to be affected by truncation artefacts or foldover.

In the case of the reactive flow experiments, undersampled propagators were acquired sampling only 41 q-space data points; this number being identified following analysis of the non-reactive (deionized water) flow experiments. Exponential sampling of points on the Nyquist grid was applied in positive q-space and mirrored in negative q-space with a one point offset to avoid acquiring symmetric data [17]. The time-constant for the exponential was chosen by linearly spacing the desired number of points between zero and the natural logarithm of the largest q-space point. The subsets of points in q-space were reconstructed using the standard MATLAB implementation of 1D linear interpolation and then Fourier transformed to produce displacement propagators. All propagators were normalised such that the area under the propagator, or total probability, was equal to 1. In addition to the undersampled propagators, 1D profiles and 2D images were acquired during the dissolution. 1D profiles were acquired in 17 s along the length of the rock core plug with 512 complex data points, 4 scans and a 100 mm field-of-view. 2D images were acquired in 2 min 31 s across the core diameter using a multi-slice RARE imaging sequence [18] with 5 equally spaced slices, each 5 mm thick with 128 × 128 pixels and a resolution of 391 μm × 391 μm. A recycle time of 5 s, an echo time of 4.86 ms; a dwell time of 5 μs and RARE-factor of 64 were used. A set of experiments comprising 1D z-profile, 2D multi-slice image and undersampled flow propagator has a total data acquisition time of ~10 min. Sets of experiments were repeated in immediate succession through the reactive flow experiment.

3. Results and discussion

The fully sampled q-space dataset of the non-reactive flow of deionized water through the rock core plug was acquired to

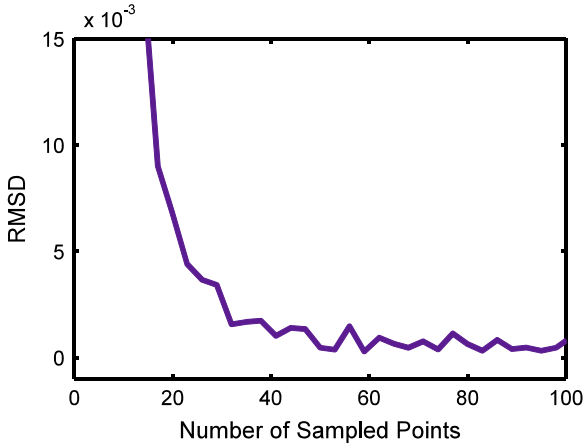

Fig. 1. A plot of the normalised root mean square deviation (RMSD) between the fully sampled and undersampled propagators as a function of the total number of q-space points used in the reconstruction.

identify the minimum number of points required for the accurate reconstruction of the propagator data. The fully sampled propagator was then undersampled to different extents, interpolated and, after Fourier transformation, compared with the fully sampled propagator. Fig. 1 shows the root mean square deviation (RMSD) between fully sampled and undersampled propagators after reconstruction for different extents of undersampling. When sampling fewer than ~20 points there is a significant loss of fidelity with the fully sampled and it was found that the RMSD reduced to less than the RMS noise value in the fully sampled propagator (1.67×10^{-3} mm^{-1}) after only 31 q-space points and no significant improvement was seen after 41 data points. Undersampling to 41 points (i.e., just 4% sampling) reduces the data acquisition time from 2 h 51 min to 6 min 51 s. Fig. 2 shows the result of undersampling to 41 points; the exponential sampling scheme retains high resolution sampling near the centre of q-space, where there are sharp features, while using a coarser sampling pattern over the extended, smooth regions. Importantly, this exponential sampling scheme also has sufficient sampling of the curvature in q-space where there is a transition between the base of the sharp feature, due to flowing spins, and the broad diffusive response.

The undersampled flow propagator measurements have been used to monitor the hydrodynamics of a hydrochloric acid solution flowing through and reacting with an Estaillades rock core plug. Fig. 3 show 2D images recorded at the beginning (Fig. 3a) and end (Fig. 3b) of the dissolution process. These images show that a general increase in porosity has occurred over the reaction, and that channels, known as 'wormholes', have been etched through the rock [19–21]. A series of 3 1D profiles acquired after 10, 120

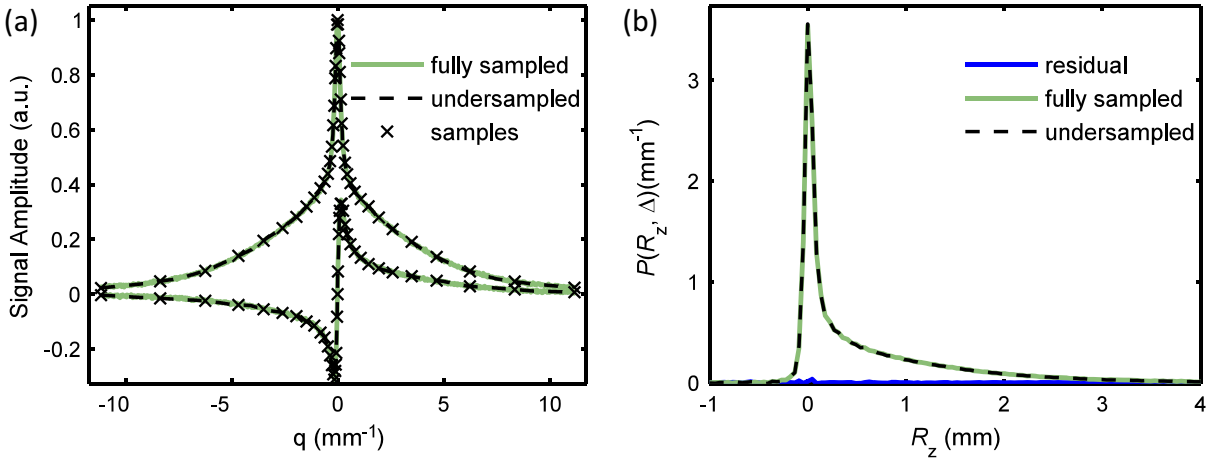

Fig. 2. Propagators for flow of deionized water through an Estaillades rock core plug. (a) The real and imaginary q-space intensity from a fully sampled propagator dataset, and an undersampled and then interpolated propagator dataset. The 41 q-space data points of the undersampled dataset are indicated by the crosses. (b) The Fourier transforms of the fully sampled, and undersampled and interpolated data shown in (a). The difference (residual) between the two is also shown.

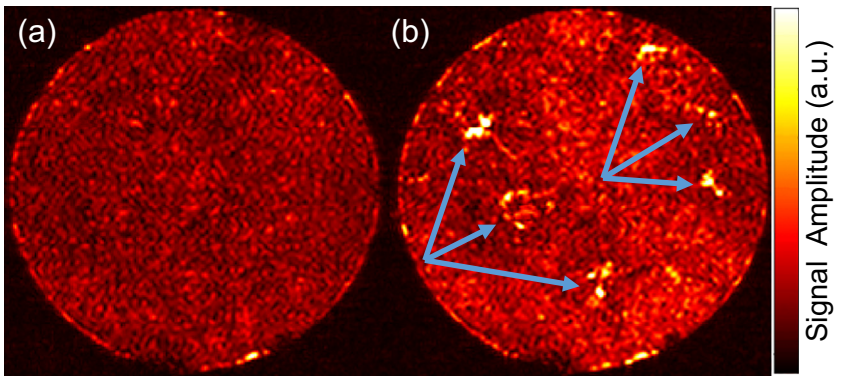

Fig. 3. 2D RARE images of the 38 mm diameter cores at: (a) the start of the dissolution process and (b) after 930 min. High signal intensity (lighter shades) indicates water-filled regions known as 'wormholes' formed through the core; these are highlighted with blue arrows. (For interpretation of the references to colour in this figure legend, the reader is referred to the web version of this article.)

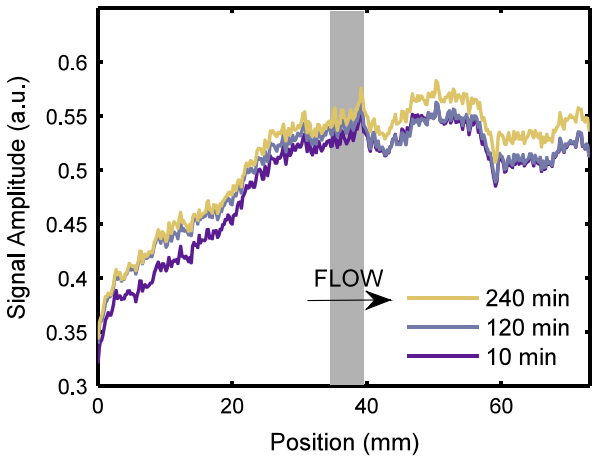

Fig. 4. NMR signal intensity profiles showing the small increase in porosity caused by the formation of wormholes advancing along the rock core plug as a function of time. The grey region highlights the 5 mm thick slice over which the 2D images in Fig. 3, and the propagators shown in Fig. 5, are recorded.

and 240 min of acid flow are displayed in Fig. 4, which shows the evolution of porosity along the rock core over the timescale of the experiment. The profiles show significant variation in signal intensity across the rock core plug even before dissolution has begun due to heterogeneities in the local porosity. As dissolution progresses Fig. 4 shows an increase in signal amplitude of ~4–5% moving along the core as a function of time at a rate of ~7 μm s^{-1}, much slower than the acid injection rate. The signal amplitude increase in the 120 min profile has just reached the shaded box region, corresponding to where the propagator measurements are taken, and has reached the end of the core in the 240 min profile. With reference to Fig. 3b the signal increase is most likely associated with the formation of the wormholes by reaction of the acid with the calcite of the rock. Despite the information contained with the 1D profiles and 2D images an understanding of how the reactive flow and associated wormhole formation influences fluid transport is not obtained. The ability to record time-resolved propagators provides important insights into this process.

Fig. 5a shows a subset of the propagator measurements recorded from the central region of the core (represented by the grey region in Fig. 4) over the course of the dissolution experiment. Initially, a broad tail of flowing spins extends to a maximum displacement of 4 mm next to a high intensity, narrow peak identifying the stagnant component centred on zero displacement. Little change in the shape of the propagator is observed up until ~90 min, which is the time at which the 1D profiles show that the signal increase approaches the region of the core at which the propagator measurements were made. As is seen from Fig. 5a, as time increases from 90 to 240 min, the intensity associated with moving spins (i.e. significant displacements) decreases. The propagator lineshape was then deconvolved into 2 components representing the fraction of spins associated with non-flowing ('stagnant') and flowing spin populations, respectively. This was achieved by fitting the peak associated with the stagnant spins using a Gaussian lineshape and subtracting this from the total lineshape. The area associated with the Gaussian lineshape is then associated with the 'stagnant' spin population and the residual intensity following subtraction is the fraction of spins that are 'flowing'. Fig. 5b shows how the proportion of stagnant and flowing spins in the propagator changes as the wormhole advances and passes through the region of measurement. Initially, ~0.7 of the spin population is identified as flowing, this value decreasing to ~0.1 after the formation of the wormhole has passed through the region of measurement. During the same time period, the fraction of signal associated with stagnant spins increases from ~0.3 to ~0.9. The time-resolved propagator measurements clearly show that as the acid flows through the rock core plug forming the wormhole, an increasing fraction of the pore space is by-passed with the spins in that pore space now associated with negligible displacement. From the image shown in Fig. 3b, the total fraction of the pore space that is comprised of wormholes is <1%. If we assume most of the fluid is passing through these wormholes, at the acid injection rate of 10 ml min^{-1} we would expect average velocities in the wormholes that extend the length of the core to be in excess of 30 mm s^{-1} and therefore be associated with displacements of ~22 mm, beyond the range shown. The signature for this flow in the propagators will be a much extended tail towards high displacements. These points will be difficult to detect due to the signal being spread over many displacement points in the propagator, and hence being of low probability. Given that the volume of the pore space associated with these high velocity

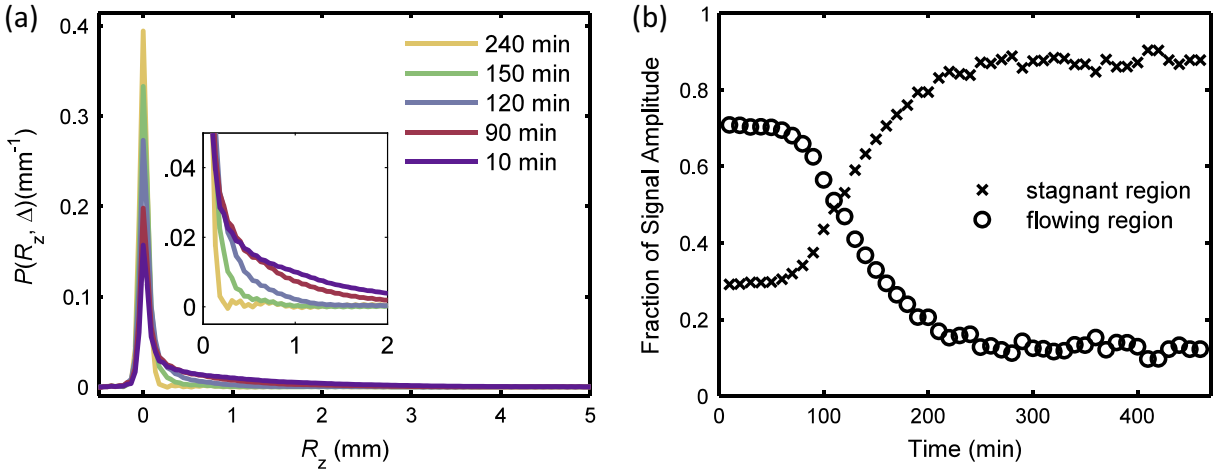

Fig. 5. (a) A plot of displacement propagators taken at 5 time points showing the change in the displacement probability distribution as a dissolution front passes through the measurement region. The inset shows a zoomed in region. (b) The fraction of the total propagator distribution associated with 'stagnant' and flowing spins, as a function of dissolution time. As the formation of the wormhole moves through the measurement region of the plug highlighted in Fig. 3, there is an increase in the 'stagnant' fluid until ~0.9 of the fluid in the measurement region is associated with non-flowing liquid.

channels (wormholes) is <1% of the volume of the core plug (based on the 2D images), the signal due to these spins is below the noise level and will not be identified in the propagator.

The time-resolved propagator measurements provide strong evidence that as acid flows into the rock core plug, it reacts with the rock along preferred paths through the plug to form a small number of dominant wormholes. As this happens the wormhole then carries the majority of the flow, by-passing the highly tortuous network of smaller pores comprising the as-received plug. It is clearly seen from Fig. 4 that acquisition of a 1D propagator employing the standard full sampling, taking ~170 min in this example, would be unable to track the evolution of wormhole formation through its effect on fluid transport. In future work this method will be used to explore how selection of both the characteristics of the reactive fluid and its flow rate influences the evolution of the void space of the rock core plug and flow through it during dissolution.

4. Conclusions

The use of undersampling combined with interpolation is a fast and simple method for the production of quantitative propagator measurements, particularly where the propagator is characterised by a well-defined narrow peak and a broad peak associated with stagnant and flowing liquid, respectively. The smooth nature of the propagator signal characteristic of flow in porous media, outside of the low q-values, lends itself to interpolation, allowing propagator measurements with high resolution in q-space to be made on the minute rather than hour timescale. Here a 2 h 51 min experiment is reduced to 6 min 51 s while maintaining an RMSD between the reconstructed and the fully sampled propagator that is below the original RMS noise level. This undersampling and interpolation of propagator measurements is applicable to flow in a wide variety of porous media, where the outer regions of q-space are smooth. In the example presented, the time resolution afforded by undersampling the propagators allowed the changes to the fluid flow caused by dissolution of the solid fraction in a rock core plug to be followed. As the wormhole is formed, increasing amounts of the fluid in the surrounding pore structure of the rock core plug becomes stagnant as the fluid in the wormhole 'channels' through the rock, by-passing the highly-interconnected (tortuous) pore network of the native rock. Such data provide new insights into reactive transport in the pore space of rock core plugs, which is important in advancing our understanding of matrix acidisation [22] and CO_2 sequestration processes [23,24].

Acknowledgments

The authors acknowledge Dr M. Benning for discussions relating to compressed sensing and the EPSRC for funding (grant numbers EP/L012251/1 and EP/K039318/1).

Data used in this paper may be accessed at http://dx.doi.org/10.17863/CAM.1239.

References

[1] E.O. Stejskal, J.E. Tanner, Spin diffusion measurements: spin echoes in the presence of a time-dependent field gradient, J. Chem. Phys. 42 (1965) 288–292.
[2] P.T. Callaghan, Translational Dynamics and Magnetic Resonance: Principles of Pulsed Gradient Spin Echo NMR, OUP, Oxford, 2011.
[3] G.A. Morris, Diffusion-ordered spectroscopy (DOSY), in: D.M. Grant, R.K. Harris (Eds.), Encyclopedia of Nuclear Magnetic Resonance, Wiley, 2002, pp. 35–44.
[4] J. Karger, W. Heink, The propagator representation of molecular transport in microporous crystallites, J. Magn. Reson. 51 (1983) 1–7.
[5] L.F. Gladden, Nuclear magnetic resonance studies of porous media, Chem. Eng. Res. Des. 71 (1993) 657–674.
[6] R.A. Waggoner, E. Fukushima, Velocity distribution of slow fluid flows in Bentheimer sandstone: an NMRI and propagator study, Magn. Reson. Imag. 14 (1996) 1085–1091.
[7] U.M. Scheven, J.G. Seland, D.G. Cory, NMR-propagator measurements in porous media in the presence of surface relaxation and internal fields, Magn. Reson. Imag. 23 (2005) 363–365.
[8] U.M. Scheven, J.G. Seland, D.G. Cory, NMR propagator measurements on flow through a random pack of porous glass beads and how they are affected by dispersion, relaxation, and internal field inhomogeneities, Phys. Rev. E 69 (2004) 021201.
[9] U.M. Scheven, D. Verganelakis, R. Harris, M.L. Johns, L.F. Gladden, Quantitative nuclear magnetic resonance measurements of preasymptotic dispersion in flow through porous media, Phys. Fluids 17 (2005) 117107.
[10] J. Mitchell, A.J. Sederman, E.J. Fordham, M.L. Johns, L.F. Gladden, A rapid measurement of flow propagators in porous rocks, J. Magn. Reson. 191 (2008) 267–272.
[11] J.L. Paulsen, H. Cho, G. Cho, Y.Q. Song, Acceleration of multi-dimensional propagator measurements with compressed sensing, J. Magn. Reson. 213 (2011) 166–170.
[12] N.M. Loening, J. Keeler, G.A. Morris, One-dimensional DOSY, J. Magn. Reson. 153 (2001) 103–112.
[13] W.C. Kittler, P. Galvosas, M.W. Hunter, Pulsed second order fields for parallel acquisition of q-space, Micropor. Mesopor. Mater. 205 (2015) 61–64.
[14] E.J. Fordham, L.D. Hall, T.S. Ramakrishnan, M.R. Sharpe, C. Hall, Saturation gradients in drainage of porous-media - NMR imaging measurements, AIChE J. 39 (1993) 1431–1443.
[15] R. Hussain, T.R.R. Pintelon, J. Mitchell, M.L. Johns, Using NMR displacement measurements to probe CO_2 entrapment in porous media, AIChE J. 57 (2011) 1700–1709.
[16] R.M. Cotts, M.J.R. Hoch, T. Sun, J.T. Markert, Pulsed field gradient methods for improved NMR diffusion measurements in heterogeneous systems, J. Magn. Reson. 83 (1989) 252–266.
[17] J.C.J. Barna, E.D. Laue, M.R. Mayger, J. Skilling, S.J.P. Worrall, Exponential sampling, an alternative method for sampling in two-dimensional NMR experiments, J. Magn. Reson. 73 (1987) 69–77.
[18] J. Hennig, A. Nauerth, H. Friedburg, RARE imaging - a fast imaging method for clinical MR, Magn. Reson. Med. 3 (1986) 823–833.
[19] C.N. Fredd, H.S. Fogler, Influence of transport and reaction on wormhole formation in porous media, AIChE J. 44 (1998) 1933–1949.
[20] G. Daccord, O. Lietard, R. Lenormand, Chemical dissolution of a porous-medium by a reactive fluid. 2. Convection vs. reaction, behaviour diagram, Chem. Eng. Sci. 48 (1993) 179–186.
[21] M.L. Hoefner, H.S. Fogler, Pore evolution and channel formation during flow and reaction in porous-media, AIChE J. 34 (1988) 45–54.
[22] C. Crowe, J. Masmonteil, E. Touboul, R. Thomas, Trends in matrix acidizing, Oilfield Rev. 4 (1992) 24–39.
[23] A. Firoozabadi, P. Cheng, Prospects for subsurface CO_2 sequestration, AIChE J. 56 (2010) 1398–1405.
[24] O. Gharbi, B. Bijeljic, E. Boek, M.J. Blunt, Changes in pore structure and connectivity induced by CO_2 injection in carbonates: a combined pore-scale approach, Energy Proc. 37 (2013) 5367–5378.